MANSOURA JOURNAL OF CHEMISTRY
Official Journal of Faculty of Science, Mansoura University, Egypt
E-mail: scimag@mans.edu.eg ISSN: 2974-4938

Phosphorus Modified Silica Nanoparticles for Efficient Removal of Basic Dyes: analytical characteristics and mechanism study

Mohammed M.H Al-Awadhi [1] , Eman Elkenawy Hassanin [2,3] and Magda A Akl [2*]

[1] *Department of Chemistry, Faculty of Education & Science, Saba Region University, Marib, Yemen*

[2] *Chemistry Department, Faculty of Science, Mansoura University 355516, Mansoura,Egypt*

[3] *Microbiology Lab.- Gastroenterology Surgical Center - Mansoura University,Mansoura, Egypt*

***Corresponding author e.** mail. magdaakl@yahoo.com (Prof. Magda A Akl)*

Received: 27/12/2022
Accepted:10/1/2023

Abstract Silica nanoparticles (SNPs) were prepared via a sol-gel method and were functionalized using cyanex921 (a Tri-octyl phosphine oxide phosphorous containing ligand) to yield the modified CY-SNPs particles. The synthesized SNPs and CY-SNPs were characterized by using SEM, FT-IR, EDS, XRD, Zeta Potential and thermogravimetric (TGA/DTA) analyses. The formed CY-SNPs were successfully used to selectively adsorb the methylene blue basic dye (MB) from real water samples in batch mode. The effect of pH, temperature, amount of sorbent, contact time, interfering ions and initial amount of MB on the adsorption capacity of CY-SNPs were examined. The chemical adsorption was shown to be the rate-determining step according to the second-order kinetic model. Additionally, the adsorption procedure showed the best fit with Langmuir model with maximum adsorption capacity of MB of 161.9 mg g^{-1}. Desorption of more than 95 % of the adsorbed dye was obtain using 5 mL of dehydrated ethanol. Also, the sorbent can be re-used for 3 times with undiminished adsorption capacity. The application, reusability indicated that CY-SNPs sorbent have a great potentiality for the removal of basic dyes from various water samples. The mechanism of adsorption of the basic dye onto the phosphorus modified Silica Nanoparticles was discussed.

keywords: Tri-octyl phosphine oxide, Cyanex921, silica, nanoparticles, basic dyes, adsorption

1.Introduction

The industrial leakage of colored dyes into the water systems is a problem of a great concern. Among all, basic dyes have been found to be the most soluble dyes that even in low concentrations, produce obvious coloration [1]. Treatment methods of dye loaded wastewater are diverse, including; membrane filtration [2,3], ion exchange [4], biological treatment [5], electrochemical methods [6], ozonation [7], coagulation [8], but the most effective and applicable is the adsorption technique [9].

Methylene blue, as a basic dye, is the water pollutant included in this work due to its excessive usage in textile industries and hence its high contribution in water pollution. Batch adsorption experiments were conducted using organically modified silica nanoparticles to investigate its performance as an adsorbent for methylene blue. Silica nanoparticles with different modifications were reported to adsorb dyes such as methyl orange [10], Congo red [11], acid red 14 [12] and methylene blue [13].

The preparation of silica nanoparticles is done via a simple sol gel method using sodium silicate and CTAB. CYANEX 921 as a phosphorus containing organic modifier is used to decorate the prepared nanoparticles. To the best of our knowledge, CYANEX compounds are mostly known as metal extractors [14,15] but few of them have been included in dye removal studies. The inclusion of CYANEX921 in such study

is a recent topic that opens up the door for more applications for such an interesting material.

The results of the batch adsorption studies reveal that the CYANEX921 modified silica nanoparticles can act as a good adsorbent for methylene blue. Further characterization of the dye loaded adsorbent was conducted using Fourier-transform infrared spectroscopy (FTIR), thermal gravimetric analysis (TGA) and differential Thermal Analysis (DTA) to confirm the adsorbent – adsorbate attachment.

2. Materials and methods

2.1.Chemicals

For preparation of nanoparticles, the following chemicals have been used; cetyltrimethyl ammonium bromide (CTAB99%) from Winlab, U.K., sodium silicate solution (5 wt.% Na_2O , 28 wt.% SiO_2, 67 wt.% H_2O) from Sigma-Aldrich, dehydrated ethanol (99.9%) from International Co., for Supp. & Med. Industries, $CYANEX_{921}$ from American Cyanamid Company.

For the adsorption studies methylene blue powder, from Nice chemicals, PvtLtd., India, was used as the dye under investigation. Stock solution of methylene blue (1000 mg/L) was prepared by stirring for 4 hours.

All chemicals were used as purchased and no further purification was performed.

2.2. Instrumentation

For characterization of the prepared nanoparticles, the following devices have been used; Scanning electron microscopy (SEM, JEOL, JSM-6510 lv, Japan and SEM, JEOL, JSM 636 OLA, Japan), Fourier transmission infrared spectroscopy (FT-IR, shimadzu, 8400s, Japan), Energy dispersive spectroscopy (EDS, Oxford X-Max 20), X-Ray Diffraction (XRD, XRD 7000, Shimadzu, Japan), Zeta Potential Analyzer (Malvern Zeta size Nano-zs90),(TGA-50 SHIMADZU / DTA-50 SHIMADZU, Japan) and UV/Vis. Spectrophotometer, Single beam (Pharmacia Biotech, UK., Ultrospec. 2000) was utilized for MB measurements.

2.3. Preparation of adsorbent

2.3.1. Preparation of silica nanoparticles

The silica nanoparticles prepared as reported in previous work [16]. Briefly, 2.6 g CTAB was dissolved in 69 g double distilled water. Afterward, 8 mL of ethanol was added to the previous solution with continuous stirring. Sodium silicate solution (9.3 g) was added to the surfactant solution and left to stir for 1 hr, the mixed solution was left for 2 hr. the solution was separated in to two phases, the phases were separated from each other and ethanol was added to the bottom phase to form a white precipitate. The solid was washed twice using ethanol, once with diluted with HCl and with distill water and dried at 30°C.

The surface dried nanoparticles was activated by further treating with HCl, afterward, the activated silica nanoparticles washed with distill water and dried at 30°C.

2.3.2.Surface modification of silica nanoparticles with Cyanex 921:

One g of the activated silica nanoparticles was suspended in 50 mL ethanol that contains 0.2 g CYANEX 921. This suspension was shaken at 100 ^{o}C till completely evaporation of 40 mL of ethanol, after that, the suspension transferred to furnace to complete dry at 35 ^{o}C.

2.3Characterization of adsorbent

Various techniques have been used to characterize the prepared native and functionalized silica nanoparticles: the surface topography and particle size information was given through sample by SEM. The crystallinity of the prepared nanoparticles was investigated by XRD technique. The elemental analysis was given by EDS) and FTIR spectroscopy was applied giving information about structure and bonds of nanoparticles under study. Zeta potential measurements were used to give knowledge about the density of the surface charge of the native and modified nanoparticles.

2.5.Adsorption and Desorption Experiments

Adsorption and desorption of MB from contaminated water were investigated using

5 mL of MB solution and 5 mg of the adsorbent in 20 mL glass containers at different pH, initial concentrations, and contact time. UV-Vis was used to measure the concentration of MB after adsorption or desorption procedures. The adsorption capacity, removal efficiency, desorption capacity, and desorption efficiency were calculated using Eqs. 1−4, respectively.

$$qe = \frac{(Ci-Ce)V}{m} \quad (1)$$

$$R\% = \frac{(Ci-Ce)}{Ci} \times 100 \quad (2)$$

$$qd = \frac{CdV}{m} \quad (3)$$

$$De\% = \frac{qd}{qe} \times 100 \quad (4)$$

where qe is the adsorption capacity (mg/g), C_i is the initial concentration of MB in solution (mg/L), Ce is the equilibrium concentration (mg/L) after adsorption, V is the volume of the solution of MB (L) and m is the mass of the adsorbent (g), % Re is the percentage of removal (%), qd is the desorption capacity (mg/g), C_d is the concentration (mg/L) of MB in the eluent after the adsorption experiment, and % D_e is the desorption efficiency (%).

2.6. Batch tests

For the batch adsorption experiments, 100 mL glass bottles each containing 0.02g of the adsorbent were used. A volume of 25 mL of different concentrations of the dye (25 – 400 ppm) were put in the bottles to examine how much the amount adsorbed of the dye is influenced by its initial concentration. The dose of the adsorbing nanoparticles was studied over the range of (0.01 - 0.1 g) using the same volume of dye and concentration of 25 ppm.

The influence of pH was examined as a separate factor over the range (3 – 11). The temperature of the suspensions was tested as an affecting factor on the adsorption process at three different temperatures (20 - 30 - 40°C).

All of equilibrium studies, other than the pH studies, were carried out at the original pH (8.0). All the suspensions were shaken on a temperature controlled water bath shaker at 125 rpm for 90min. The loaded nanoparticles were separated in order to characterize their properties and to measure the amount of MB left in the out coming solution. UV- visible absorbance was used to determine the amount of the MB left at λ_{max} = 664nm and amounts of the adsorbed dye (q_e) and the amount of dye removed (Removal %) were calculated using equations (1&2).

The rate of the MB adsorption was investigated as an important factor affecting MB removal. A series of 100 mL glass bottle each contains 0.02 g of the nanoparticles adsorbent and 25 mL of MB solution of 100 mg L^{-1} concentration were used to detect the minimum time needed for the adsorption of the MB to reach equilibrium at the original pH (8.0). The glass bottles were placed on a temperature controlled water bath shaker at 125 rpm at 30°C and samples of approximately 2mL were taken from the suspension at various time intervals of the adsorption process. The concentration of the MB in effluent solutions were analyzed as mentioned before and the amounts of the adsorbed dye (q_e) were calculated and plotted against time.

2.7. Sample analysis

Surface natural water samples were collected from the Nile River, sea water and tap water samples were filtered using a sintered glass G4 filter and acidified with conc. HNO3 to pH ~2.The organic matter was digested before the adsorption procedure using 0.5 - 1.0 g of $K_2S_2O_8$. 50 mg of CY-SNPs was added to a series of transparent stoppered bottles that contain various amounts of MB (0.0, 50.0 and 100.0 μgl^{-1}) at 25°C and pH (8.0). The stoppered bottles were shaken at 150 rpm on an equilibrated shaker for 30 min; then filtered. To the filtrate another 30mg of CY-SNPs were added and the pH was controlled again. The samples were shaken again for 15 min and filtered. Both residues were gathered and the concentration of MB in the filtrate was determined spectrophotometrically as previously mentioned.

Results and Discussion

3.1.Characterization

Scanning electron microscopy (SEM)

The morphology of the silica nanoparticles and $CYANEX_{921}$ modified silica (Fig.1c&d) were investigated. The SEM images indicated that the activated silica nanoparticles own spherical morphology with average particle size (~33 nm) as shown in Fig.1a&b. By modification of silica nanoparticles with $CYANEX_{921}$ we observed an increase in the particle size of the $CYANEX_{921}$ modified silica (~90 nm) (Fig.1c&d), this is may be attributed to agglomeration of silica nanoparticles caused by modification process.

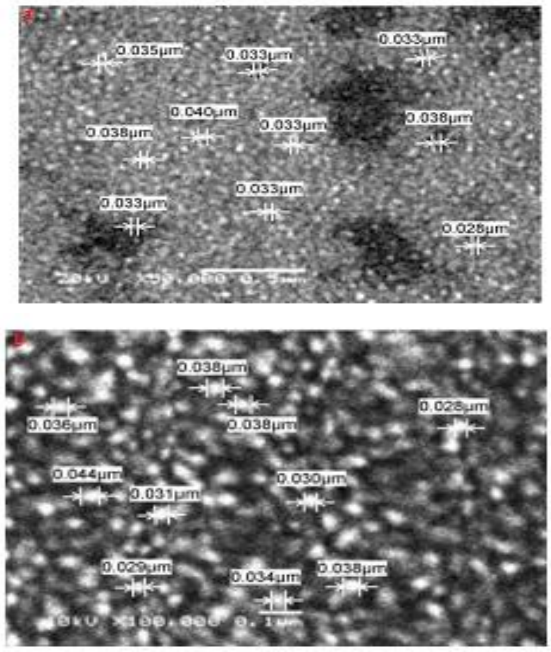

Fig.1. SEM photographs of Silica nanoparticles a&b) before loading of CYSNPs

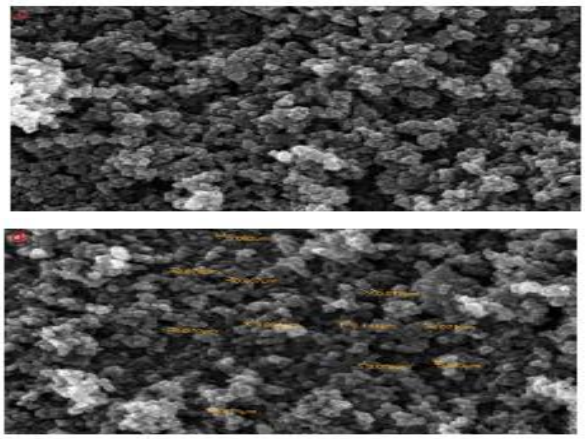

Fig.1. SEM photographs of Silica nanoparticles c & d) after loading of CYANEX 921

Energy dispersive spectroscopy (EDS)

The EDS analysis of silica nanoparticles was acquired using, Oxford X-Max 20, a component attached to the SEM instrument. The peaks recorded around 1.9 Kv and 0.5 Kv crossponding to the binding energies of Si and O, respectively, as shown in Fig. 2a, which confirms the presence of silicon and oxygen with content around the stoichiometric composition. Moreover, the ESD analysis for $CYANEX_{921}$ modified silica nanoparticles has with additional peak at around 2.1 Kv referring to phosphorous from the $CYANEX_{921}$ moiety, additionally, the carbon was present at higher percent regarding to content of carbon from the organic modifier, see Fig. 2b.

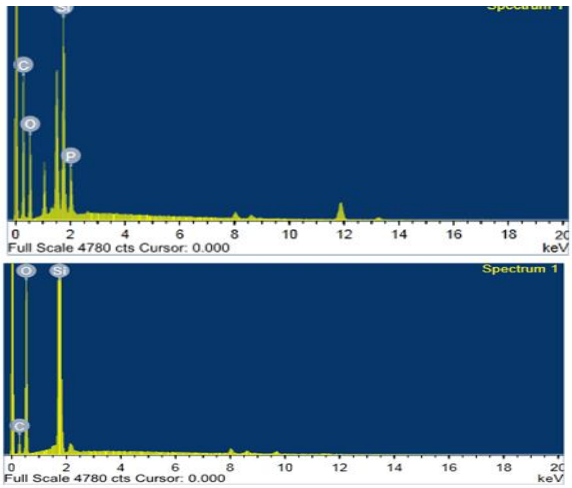

Fig. 2. EDS analysis of Silica and Silica load by CYANEX 921

Table 1 The EDS findings of the prepared SNPs and CY-SNPs

Mnbv		
Atomic %	**Weight %**	**Element**
25.04	17.83	C K
59.49	56.37	O K
15.51	25.81	Si K
CY-SNPs		
Atomic %	**Weight%**	**Element**
63.88	54.83	C K
29.87	33.86	O K
2.34	3.81	Na K
3.12	6.22	Si K
0.79	1.74	P K

Fourier transmission infrared spectroscopy (FT-IR)

The FTIR spectra of the silica nanoparticles, CYANEX921 modified silica and CYANEX921 modified silica-MB complex were shown in Fig.3.

The FTIR spectra of the silica nanoparticles presented the characteristics peaks related to the silica intense broad band around 3300–3500 cm^{-1} (O-H stretching vibration), The band at ~1641 cm^{-1} (bending vibration of molecular H_2O), ~1079 cm^{-1} (asymmetric vibration of Si-O bond), intense and broad band appearing at ~1033–1220 cm^{-1} (antisymmetric stretching vibrations of Si-O-Si siloxane bridges) and intense narrow band at 802 cm^{-1} (asymmetric vibration of Si-OH bond).

After modification of silica nanoparticles with Cyanex 921 the intensities of the peaks at 3300–3500 cm^{-1}, ~1641 cm^{-1} and 802 cm^{-1} were reduced which explained that involving of the O-groups in the modification process.

On the other hand, peaks 2854 and 2921 cm^{-1} were appeared due to stretching of C—H bonds from the alkyl chains [17.].

After adsorption of MB by the CYANEX921 modified silica, the FTIR of the adsorbent CYANEX921 modified silica-MB complex showed that most of the bands that are characteristic of the sorbent were kept the same, some of the bands were shifted, some were split and others appeared after the adsorption process. On focus, bands appeared such as the band detected at 1650 cm^{-1} which is assigned for the vibration of the $N^{+}(CH_3)_2$ bond [18], The band detected at 1222 cm^{-1} which is assigned for the Vibrations of heterocycle skeleton [18], the band at 1542 cm^{-1} corresponds to the C-N and C-C vibrations of the MB heterocycle [19].

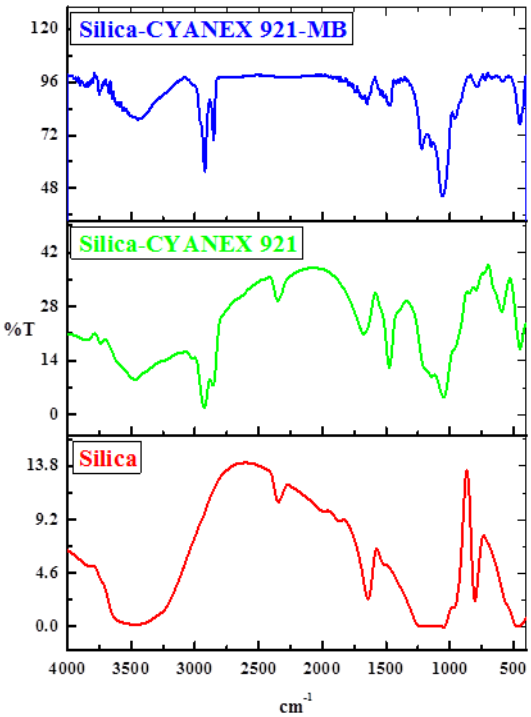

Fig. 3. FT-IR spectra of Silica, CY-SNPs and MB-CY-SNPs loaded complex.

X-Ray Diffraction (XRD)

XRD analysis was performed to investigate the crystalline and/or amorphous nature of CYSNPs. As shown in Figure 4, the sharp and broad diffraction peak at 2θ = 20 was recorded. This result can be attributed to the typical crystalline regions of the CYSNPs, which are established through intramolecular and intermolecular H-bonding interactions.

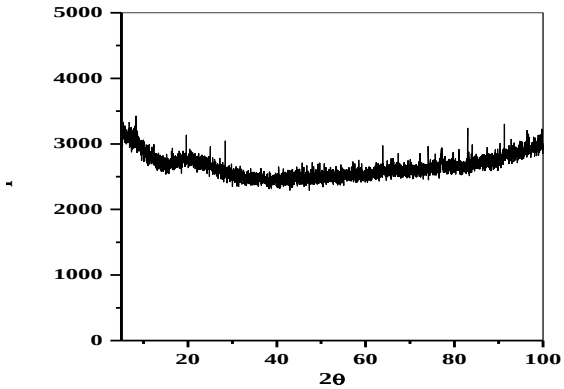

Fig. 4. XRD-pattern of Silica nanoparticles

Zeta Potential

Zeta potential measurements were determined for both native and modified nanoparticles, as presented in Fig. 5. The values of the potential were found to be -19.6 mV for the silica nanoparticles and 40.7mV for the $CYANEX_{921}$ modified silica nanoparticles. The high potential at the surface indicates the low tendency of the nanoparticles to aggregate.

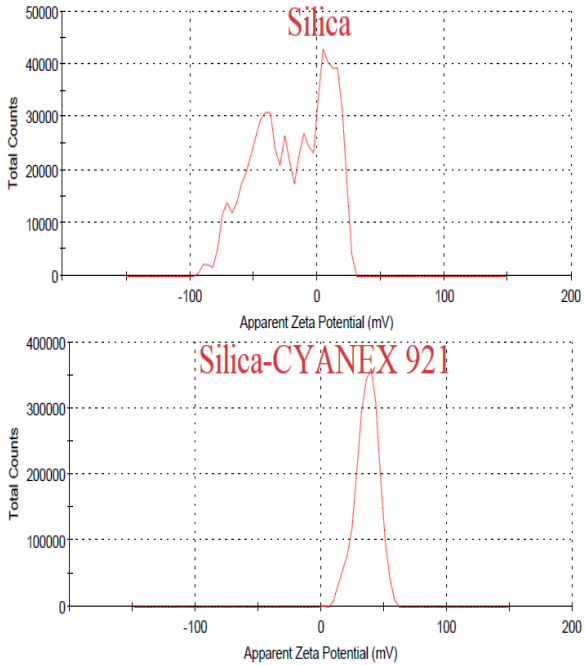

Fig. 5. Zeta potential of Silica and CY-SNPs

Thermo- gravimetric measurements (TGA and DTA)

The thermal behaviors of the dye loaded adsorbent were examined using TGA and DTA. Fig. 6 shows the curves obtained for the dye loaded adsorbent. The thermal study

1001.89 °C). The thermal degradation shows three main decomposition stages and they are 39.30 C, 114.9 °C and 260.12 °C with a total weight loss of 61.54 %.

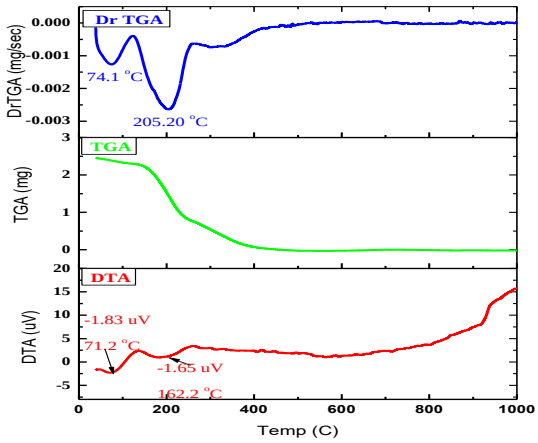

Fig. (6): DTA & TGA curves for the CY-SNPs loaded with MB

3.1.Adsorption studies

3.1.1.Influence of pH

The pH of sample is an important factor in adsorption procedures because it influences the surface charge of the adsorbent, and the degree of ionization and speciation of adsorbate [13]. The effect of initial pH on the separation of MB by CYANEX$_{921}$ modified silica NPs is illustrated in Fig.7, by plotting the values of the amount of dye adsorbed against their corresponding pHs. From the Fig.7, it can be noticed that the adsorption procedure is less favorite in acidic mediums and the adsorbed amount of the MB increase with further increase in the pH value to reach maximum adsorption at pH equals 8.

However, the further increase in the pH value present no significantly alter in the adsorbed amount of the MB-dye. The dependence of adsorption of MB-species over CYANEX921 modified silica NPs on pH, can be explained on bases at lower pH the available active sites on the adsorbent could be partially occupied by the hydrogen ions, so less sites will be available for MB molecules.

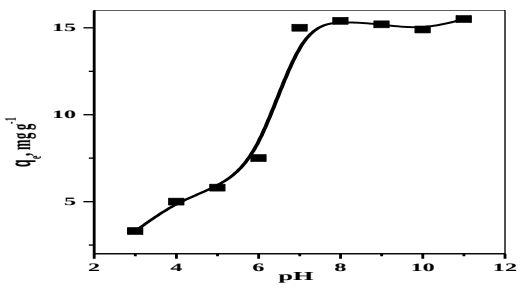

Fig. 7. Effect of the pH values on adsorption capacity of MB by CYSNPs. (Conditions: C_o = 25 mg/l, T=30°C; adsorbent dose = 0.02 g/25 ml; time = 90min)

3.1.1. Influence of sorbent dose

The effect of adsorbent mass on adsorption of MB by CYSNPs is shown in Fig. 8. As it can be noticed, the increase in the adsorbent dose is in favor of dye separation. When the adsorbent mass increased from 0.01g to 0.05 the percent MB separated increases from 36.5% to 79.7 % and the maximum removal of MB is attained using 0.09g of adsorbent.

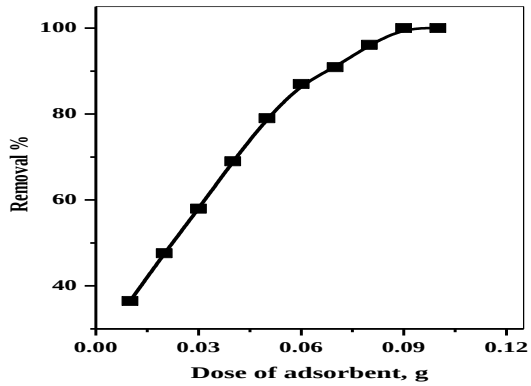

Fig. 8. Effect of sorbent dosage on the removal of MB by CYSNPs.

(Conditions: T=30°C; C_o = 25 mg/l; time = 90min).

3.1.1.Influence of initial dye concentration

As it can be seen from Fig. 9a the increase in the initial dye concentration enhances the amount of dye adsorbed until 150ppm. After 150 ppm, the increase in the initial MB amounts results in no more increase in the amount adsorbed. Such positive effect can

be attributed to the increased strength of the concentration gradient at high concentrations. This increase continues until all the sites available at the adsorbent are occupied

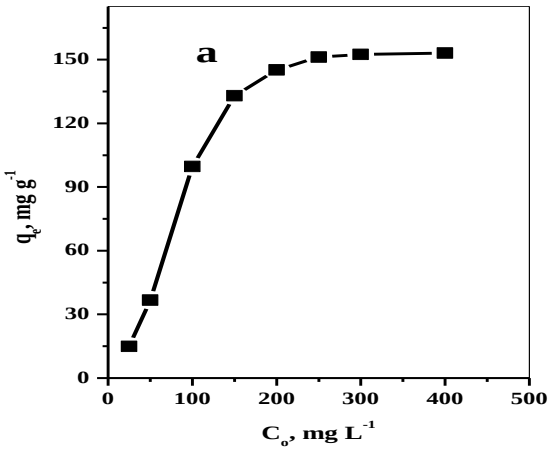

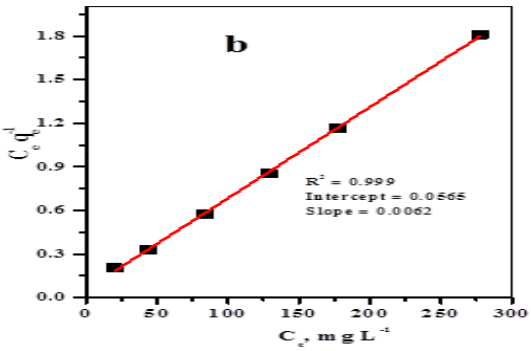

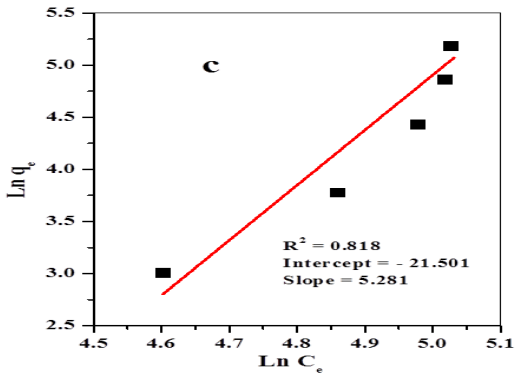

Fig. 9 a) Effect of initial MB concentration on the uptake of MB by CYSNPs, b) Langmuir isotherm and c) Freundlich isotherm (Conditions: T=30°C; adsorbent dose = 0.02 g/25 ml; time = 90min).

3.2.4. Adsorption isotherms

Freundlich and Langmuir isotherms are best frequently applied models to describe the equilibrium relationship between adsorbent and the adsorbate in solution. The mathematical linear formulas of the isotherms at steady temperature are expressed as follow:

Langmuir isotherm:

$$\frac{C_e}{q_e} = \frac{1}{Q_o K_l} + \frac{C_e}{Q_o} \quad (5)$$

$$R_l = \frac{1}{1 + K_l C_o} \quad (6)$$

Where q_e is the amount of MB adsorbed (mg/g) onto the adsorbent used, C_e is the residual concentration of MB(mg/L) and k_l and Q_o are constants related to energy of adsorption (L/mg) and adsorption capacity (mg/g) respectively.

The dimensionless constant R_L was calculated using Eq.6, to indicate the favorability of the isotherm, where K_l was the Langmuir constant and C_o was the highest initial MB concentration (mg/L). The value of R_L indicates the type of the isotherm to be either unfavorable ($R_L > 1$), linear ($R_L = 1$), favorable ($0 < R_L < 1$) or irreversible ($R_L = 0$).

The R is ($0 < 0.053 < 1$) denoting that the adsorption of MB onto CYSNPs is a favorable process.

Freundlich isotherm

$$\ln q_e = \ln K_f + \frac{1}{n} \ln C_e \quad (7)$$

Where, k_f and n are empirical constants of the Freundlich isotherm, q_e is the concentration of MB adsorbed (mg/g) onto CYSNPs and C_e is the residual amount of MB(mg/L). The magnitude of the component (n) gave an indication of the favorability and K_f is an indication of the capacity of the adsorption.

The statistical correlation coefficient R^2 was calculated in order to measure the strength of the linear relationship in both of the isotherms. The Langmuir and Freundlich isotherms for the adsorption of MB onto $CYANEX_{921}$ modified silica NPs are shown in Figs 9 b & c. The isotherm constants and the correlation coefficients for both models were presented in Table (2). The statistical correlation coefficient R^2 (0.999) value for the linear plot of the Langmuir equation is greater than that of Freundlich isotherm (R^2 = 0.8182) denoting that the adsorption of

MB is best fit with the Langmuir isotherm model.

Table 2: Isotherm model parameters and correlation coefficients at 30° C

Model	parameters	values	R^2
Langmuir	**Q_o**, maximum monolayer adsorption capacity (mg/g)	161.29	0.9994
	K_L, Langmuir constant (L/mg)	0.109	
	R_L, separation factor	0.053	
Freundlich	**K_F**, Affinity	4.599x 10^{-10}	0.8182
	1/n, Freundlich exponent	5.281	
	B, heat of adsorption constant (J/mol)	19.936	

3.2.5. Influence of contact time

The effect of contact time on the maximum adsorption capacity of MB is shown in Fig.

10a, As it can be noticed, the contact time required for MB solution to reach equilibrium is about 90 min; the amount of MB adsorbed increases with increasing the time till 90 min when it starts to almost become constant, that's when no more MB can be adsorbed at the surface of the sorbent.

3.2.6. Adsorption kinetics

Both pseudo1st order and 2nd order kinetic models were applied to describe the experimental data obtained from the process of MB removal. The linear formulas of the two models are given by Eqs. 8&9

The pseudo-1st order is given by:

$$\log(q_e - q_t) = \log q_e - \frac{K_1 t}{2.303} \quad (8)$$

Where q_e is the adsorption uptake of MB at time t (mg/g) and k(1/min) is the rate constant of the pseudo-first-order adsorption.

The pseudo-2nd -order is given by:

$$\frac{t}{q_t} = \frac{1}{K_2 q_e^2} + \frac{t}{q_e} \quad (9)$$

Where k_2 (g mol^{-1} min^{-1}) is the rate constant of the pseudo- second order adsorption. It can be seen from Table (3) that the value of R^2 for the pseudo- 2nd order model is higher that of pseudo- 1st order model. These data suggest that the adsorption process of MB onto CYSNPs can be better described by a pseudo-second order kinetic model.

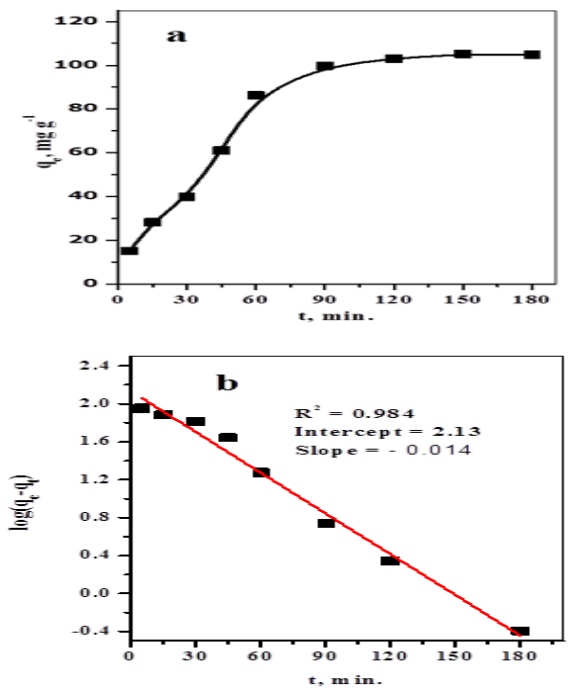

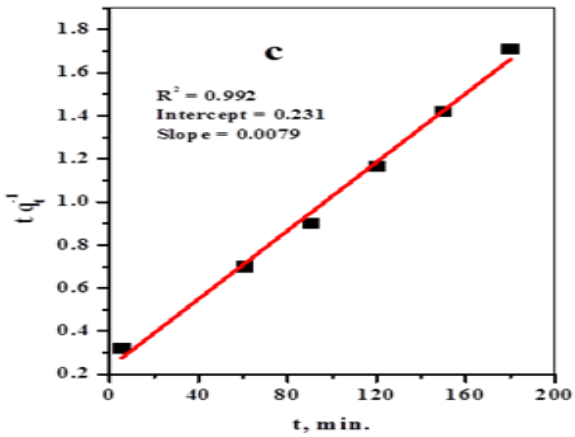

Fig. 10. a) Effect of contact time on the uptake of MB by CYSNPs, b) pseudo first order model and c) pseudo secondorder model. (Conditions: T=30°C; adsorbent dose = 0.02 g/25 ml; dye concentration 100ppm).

Table 3: Calculated parameters of the pseudo 1st -order and pseudo 2nd- order kinetic models of the adsorption of MB by CY-SNPs

Pseudo 2nd -order		
K_2 (g $mg^{-1}min^{-1}$)	q_{ecal}(mg /g)	R^2
2 x 10^{-4}	135	0.995
Pseudo 1st - order		
K_2 (g $mg^{-1}min^{-1}$)	q_{ecal}(mg /g)	R^2
-0.032	105	0.884

3.2.7. Influence of temperature

The influence of temperature on the adsorption was examined under at temperatures 20, 30 and 40°C. The effect of temperature on adsorption of MB onto CY-SNPs is shown in Table (4). It could be clearly obvious that, the values of the maximum adsorption capacity (q_e) increase with increasing temperature, suggesting that the nature of the adsorption reaction was endothermic. As the temperature raised from 20°C to 40 °C, the maximum amounts of MB removed by CY-SNPs was increased from 66.25 to 121.37 mg/g. This behavior might be attributed to one of two possibilities; the increase of the intraparticle

migration of MB molecules to the active sites of the NPs, or the temperature enhancement of the chemical interaction between the adsorbent and the adsorbate.

Table 4 Effect of temperature on maximum adsorption capacities of MB by CY-SNPs(Conditions: C_o = 100 mg/l; time = 90min; adsorbent dose =0.02g/25mL).

Temperature (^oC)	%Removal (%)	q_{max}(mg/g)
20	53.02	66.25
30	79.76	99.7
40	97.09	121.37

3.2.8. Desorption and reusability studies

A promising adsorbent is needed to have not only high adsorption capacity but also regeneration ability for reuse. Dehydrated ethanol was used as desorbing agent for regeneration of the CY-SNPs. The regenerated adsorbent is further washed with double distilled water. Also, the adsorption capacity in the second cycle is approximately similar to that of first cycle, this indicates that treatment of CY-SNPs with dehydrated ethanol provides a good way of regeneration of dye loaded adsorbent.

To test the reusability of the CY-SNPs, the subsequent adsorption-desorption procedure was performed for three times using the same adsorbing and desorbing conditions.

Reloading efficiency = amount adsorbed after reuse / amount adsorbed before reusex100

Table (5) Adsorption-desorption cycles.

Cycle	Adsorption capacity (mg/g)	Removal(%)	Reloading efficiency (%)
First cycle	7.81	96.1	99.9
Second cycle	7.80	96.0	99.87
Third cycle	7.35	94.2	94.23

3.1. Proposed mechanism of Adsorption

The adsorption process usually supports the mixed mechanisms of physisorption and chemisorption mechanism. The physisorption mechanism always considered the adsorption process done through electrostatic interactions between +ve charges of dyes and -ve surface of adsorbents which are usually full of donating electrons groups such as -OH group, -NH2 group, -C=O group…. etc. On the other hand, the chemisorption mechanism is explained as ion exchange or chelation interaction one.

In the present study, adsorption of the MB dye is supposed to be due to mixed physisorption and chemisorption mechanism. The physiosorption mechanism is supported by electrostatic interaction between +vely charged groups of the MB dye with -vely charged groups available on the CYSNPs surface.

On the other hand the chemsorption mechanism is supported by the following findings:

1. The data obtained from kinetic section clarify that CYSNPs adsorbents obeyed pseudo second order model which improved the chemisorption pathway.

2. These data agree with results of isotherm studies which indicated complete following of CYSNPs adsorbents to the mono-layer Langmuir model against other model.

3. Similarly, new functional groups appeared at FTIR chart due to the chemical treatment for CYSNPs push in the way of

chelating interaction between cationic dye and CYSNPs adsorbent.

According to the possibilities mentioned above, these interactions were responsible for enhancing the adsorption process of MB on the CYSNPs surface.

3.4. Applications

The optimized experimental conditions were applied to real water samples to investigate the efficiency of CYSNPs for the adsorption of cationic dyes. The analytical samples were tap water in our lab in Mansoura University, Nile river water in Mansoura City and Sea water in Alexandria City. The analytical results are as shown in Table 6. The MB dye was not found in all of the samples. The recoveries were examined in the samples in which given amounts of MB were spiked. The recoveries obtained were in the range of 98.00- 99.42%. These results indicate that CYSNPs method could be successfully used for the determination of cationic dyes in real water samples.

3. Conclusion

Here in, were reported preparation, characterization of efficient adsorbent (CYANEX$_{921}$ modified silica NPs) using simple impregnation step of silica NPs and tri-

octyl phosphine oxide and its application in removing of MB as a cationic pollutant model. The experimental data showed that the MB adsorbed on the $CYANEX_{921}$ modified silica NPs surface as monolayer according to Langmuir isotherm. Moreover, it was found that the kinetics results were best fitted with the pseudo second order model. The maximum capacity of MB onto $CYANEX_{921}$ modified silica NPs is comparable with other previously reports. Table7.

Table 6 Analytical results of recovery of MB (µg ml^{-1}) in real water samples using CY.SNPs. (n=5)

Sample	spiked (µgmL^{-1})	Measured(µgmL^{-1})	Recovered(µgmL^{-1})	Recovery (%)	RSD (%)
Tap water	0.00	0.00	0.00	0.00	--
	50	**0.5**	49.5	99.0	1.7
	100	1.8	98.2	98.2	1.8
Nile water	0.00	0.00	0.00	0.00	00
	50	0.93	49.07	98.14	2.10
	100	2	98	98	1.8
Sea water	0.00	0.00	0.00	0.00	--
	50	0.33	49.67	99.34	1.98
	100	1.27	98.73	98.73	1.65

Table (7): Maximum capacity of monolayer adsorption (q_{max} calculated from Langmuir model) of MB adsorbed by various adsorbents

	Dose (g/L)	Temp(K)	C_0 (mg/L)	q_{max} (mg/g)	References
CY-SNPs	0.8	303	25-400	161.29	This study
Graphene	0.5	293	20–120	153.85	[21]
hydrogel beads of poly(vinyl alcohol)-sodium alginate-chitosan-montmorillonite	1.0	303	10-70	137.15	[22]
CH–Mt/PANI	5.0	298	--	111	[23]
Gl-crosslinked PVA/VC-MWCNTs composites	8.0	298	10-300	16.8	[24]
Raw activated carbon	2.0	303	(200–600	178.25	[25]
Fe–Ce-AC	2.0	303	(200–600	255.76	[25]
SDS surface-modified $ZnFe_2O_4$ nanoparticles	0.1	288	40–100	699	[26]
SDS surface-modified ZnFe2O4 nanoparticles	0.5	288	5-60	115.34	[26]
CoFe2O4/MWCNT composites	1.0	298	3–15	11.10	[27]
Activated carbon/cellulose	--	308	20-100	103.7	[28]

References

1. Maheria, K. C., &Chudasama, U. V. (2007). Sorptive removal of dyes using titanium phosphate. Industrial & Engineering Chemistry Research, **46(21),** 6852-6857.
2. Lau, W. J., & Ismail, A. F. (2009). Polymeric nanofiltration membranes for textile dye wastewater treatment: preparation, performance evaluation, transport modelling, and fouling control—a review. Desalination, **245(1-3),** 321-348.
3. Mo, J. H., Lee, Y. H., Kim, J., Jeong, J. Y., &Jegal, J. (2008).Treatment of dye aqueous solutions using nanofiltration polyamide composite membranes for the dye wastewater reuse. Dyes and Pigments, **76(2),** 429-434.
4. Karcher, S., Kornmüller, A., &Jekel, M. (2002). Anion exchange resins for removal of reactive dyes from textile wastewaters. Water Research, **36(19),** 4717-4724.
5. Bhatia, D., Sharma, N. R., Singh, J., &Kanwar, R. S. (2017). Biological methods for textile dye removal from wastewater: A review. Critical Reviews in Environmental Science and Technology, **47(19),** 1836-1876.
6. Vlyssides, A. G., Papaioannou, D., Loizidoy, M., Karlis, P. K., &Zorpas, A. A. (2000).Testing an electrochemical

method for treatment of textile dye wastewater. Waste management, **20(7),** 569-574.

7. Koch, M., Yediler, A., Lienert, D., Insel, G., &Kettrup, A. (2002).Ozonation of hydrolyzed azo dye reactive yellow 84 (CI). Chemosphere, **46(1),** 109-113.
8. Liang, C. Z., Sun, S. P., Li, F. Y., Ong, Y. K., & Chung, T. S. (2014). Treatment of highly concentrated wastewater containing multiple synthetic dyes by a combined process of coagulation/flocculation and nanofiltration. *Journal of Membrane Science*, **469,** 306-315.
9. 9. Yagub, M. T., Sen, T. K., Afroze, S., & Ang, H. M. (2014). Dye and its removal from aqueous solution by adsorption: a review. Advances in colloid and interface science, **209,** 172-184.
10. Liu, J., Ma, S., & Zang, L. (2013). Preparation and characterization of ammonium-functionalized silica nanoparticle as a new adsorbent to remove methyl orange from aqueous solution. Applied Surface Science, **265,** 393-398.
11. Das, S. K., Khan, M. M. R., Parandhaman, T., Laffir, F., Guha, A. K., Sekaran, G., & Mandal, A. B. (2013). Nano-silica fabricated with silver nanoparticles: antifouling adsorbent for efficient dye removal, effective water disinfection and biofouling control. Nanoscale, ***5*(12),** 5549-5560.
12. Mahmoodi, N. M., Khorramfar, S., &Najafi, F. (2011). Amine-functionalized silica nanoparticle: Preparation, characterization and anionic dye removal ability. Desalination, **279**(1-3), 61-68.
13. Dutta, D., Thakur, D., &Bahadur, D. (2015). SnO2 quantum dots decorated silica nanoparticles for fast removal of cationic dye (methylene blue) from wastewater. *Chemical Engineering Journal*, **281**, 482-490.
14. Awwad, N. S., El Afifi, E. M., & El Reefy, S. A. (2005).Solvent Extraction of Uranium (VI) by CYANEX 301/CYANEX 921 and their Binary Mixtures from Aqueous HNO 3 and H 2 SO 4 Media. Equilibrium, ***87*(79.0),** 58-0.
15. Navarro, R., Gallardo, V., Saucedo, I., &Guibal, E. (2009). Extraction of Fe (III) from hydrochloric acid solutions using Amberlite XAD-7 resin impregnated with trioctylphosphine oxide (Cyanex 921). Hydrometallurgy, **98**(3-4), 257-266.
16. H F Aly, M A Akl, Hesham M A Soliman, Aref M E AbdEl-RahmanAbd-Elhamid, Nano (2020) silica particles loaded with CYANEX-921 for removal of iron(III) from phosphoric acid, Indian *Journal of Chemical* Technology, **27** 303-310.
17 Abdien, H. G., Cheira, M. F., Abd-Elraheem, M. A., El-Naser, T. A. S., &Zidan, I. H. (2016). Extraction and pre-concentration of uranium using activated carbon impregnated trioctyl phosphine oxide. Elixir Applied Chemistry, **100**, 3462-43469
18. Ovchinnikov, O. V., Evtukhova, A. V., Kondratenko, T. S., Smirnov, M. S., Khokhlov, V. Y., &Erina, O. V., (2016) Manifestation of intermolecular interactions in FTIR spectra of methylene blue molecules. Vibrational Spectroscopy, **86** 181-189.
19. Ovchinnikov, O. V., Chernykh, S. V., Smirnov, M. S., Alpatova, D. V., Vorob'Eva, R. P., Latyshev, A. N., ... & Lukin, A. N., (2007) Analysis of interaction between the organic dye methylene blue and the surface of AgCl (I) microcrystals. *Journal of Applied Spectroscopy*, **74(6)** 809-816.
20. Ovchinnikov, O. V., Chernykh, S. V., Smirnov, M. S., Alpatova, D. V., Vorob'Eva, R. P., Latyshev, A. N., ... & Lukin, A. N., (2007) Analysis of interaction between the organic dye methylene blue and the surface of AgCl (I) microcrystals. *Journal of Applied Spectroscopy*, **74(6)** 809-816.
21. Liu, T., Li, Y., Du, Q., Sun, J., Jiao, Y., Yang, G. & Wu, D. (2012). Adsorption of methylene blue from aqueous solution by graphene. Colloids and Surfaces B: Biointerfaces, **90**, 197-203.
22. Wang, W., Zhao, Y., Bai, H., Zhang, T., Ibarra-Galvan, V., & Song, S. (2018). Methylene blue removal from water using the hydrogel beads of poly (vinyl alcohol)-sodium alginate-chitosan-

montmorillonite. Carbohydrate polymers, **198**, 518-528.
23. Minisy, I. M., Salahuddin, N. A., & Ayad, M. M. (2021). Adsorption of methylene blue onto chitosan–montmorillonite/polyaniline nanocomposite. Applied Clay Science, 203, 105993.
24. Mallakpour, S., & Rashidimoghadam, S. (2019). Poly (vinyl alcohol)/Vitamin C-multi walled carbon nanotubes composites and their applications for removal of methylene blue: Advanced comparison between linear and nonlinear forms of adsorption isotherms and kinetics models. Polymer, **160**, 115-125.
25. Cheng, S., Zhang, L., Ma, A., Xia, H., Peng, J., Li, C., & Shu, J. (2018). Comparison of activated carbon and iron/cerium modified activated carbon to remove methylene blue from wastewater. *Journal of environmental sciences*, **65**, 92-102.
26. Zhang, P., Lo, I., O'Connor, D., Pehkonen, S., Cheng, H., & Hou, D. (2017). High efficiency removal of methylene blue using SDS surface-modified ZnFe2O4 nanoparticles. *Journal of colloid and interface science*, **508**, 39-48.
27. Farghali, A. A., Bahgat, M., El Rouby, W. M. A., & Khedr, M. H. (2012). Decoration of MWCNTs with CoFe2O4 nanoparticles for methylene blue dye adsorption. *Journal of solution chemistry*, **41(12)**, 2209-2225.
28. Somsesta, N., Sricharoenchaikul, V., & Aht-Ong, D. (2020). Adsorption removal of methylene blue onto activated carbon/cellulose biocomposite films: equilibrium and kinetic studies. Materials chemistry and physics, 240, 122221.